agronomy

Article

Influence of Crop and Land Management on Wind Erosion from Sandy Soils in Dryland Agriculture

Heleen C. Vos [1,*], Isabel G. Karst [1], Frank D. Eckardt [2], Wolfgang Fister [1] and Nikolaus J. Kuhn [1]

[1] Department of Environmental Sciences, University of Basel, 4056 Basel, Switzerland; isabelgloria.karst@unibas.ch (I.G.K.); wolfgang.fister@unibas.ch (W.F.); nikolaus.kuhn@unibas.ch (N.J.K.)
[2] Department of Environmental and Geographical Sciences, University of Cape Town, Cape Town 7701, South Africa; frank.eckardt@uct.ac.za
* Correspondence: heleen.vos@unibas.ch

Abstract: Minimizing wind erosion on agricultural fields is of great interest to farmers. There is a general understanding that vegetation can greatly minimize the wind erosion taking place. However, after harvest, a low vegetation cover can be inevitable, whereby the amount of stubble that remains on a field is dependent on the crop type and land management. This study aims at quantifying the vulnerability to wind erosion of different crops, and the possibility to predict the vulnerability based on high precision aerial images. The study area was the semi-arid Free State, which holds large intensive agriculture on sandy soils. These croplands have been identified as the largest emitter of dust in South Africa. The main crop in the region is maize, but also sunflower, peanut and fallow fields are common land-use types. On these fields, the horizontal sediment flux, the saltation threshold, and aerodynamic roughness length were measured, and the soil cover was assessed using Unmanned Aerial Vehicle (UAV) imagery. The results showed a strong relationship between the soil cover and the sediment flux, whereby fallow and groundnut fields have the highest wind erosion risk. These results emphasize the great importance of soil cover management to prevent wind erosion.

Keywords: wind erosion; land management; soil cover; UAV image analysis; sediment flux

Citation: Vos, H.C.; Karst, I.G.; Eckardt, F.D.; Fister, W.; Kuhn, N.J. Influence of Crop and Land Management on Wind Erosion from Sandy Soils in Dryland Agriculture. *Agronomy* **2022**, *12*, 457. https://doi.org/10.3390/agronomy12020457

Academic Editors: Bořivoj Šarapatka, Miroslav Dumbrovský and Jana Podhrázská

Received: 13 December 2021
Accepted: 7 February 2022
Published: 12 February 2022

1. Introduction

Wind erosion is known for the disastrous effects it can have on agricultural lands due to the damage it can bring to the crops by saltation [1,2] and the degrading effect on the soil, because of the removal of nutrients and topsoil [3–7]. The dust that is transported from the fields can become part of the global chemical flux and can, furthermore, have offsite effects on human health and climate. Wind erosion is especially a problem in semi-arid and arid regions [8], where fields are most vulnerable after harvest, when the soil cover from plants or residue is low. The total global wind erosion is estimated to be s 6577 t km^{-2} yr^{-1} [9]. During these wind erosion processes, roughly 500 to 3320 Tg yr^{-1} of dust is being emitted [10]. The dust emission from anthropogenic areas has been estimated to be 10% to 25% of the total dust load, whereby the contribution of anthropogenic dust differs greatly per region [8,11].

The most important method for preventing wind erosion from agricultural fields is the maintenance of a residue and vegetation cover [12–18]. The erodibility of a surface can furthermore be influenced by the presence of a soil crust that increases cohesion and thus in turn by the tillage operations that disturb the crust [19–21]. The influence of soil cover on wind erosion can be expressed as a ratio of wind erosion from a surface with vegetation to a surface without vegetation. Exact exponential relationships have been developed by Fryrear [22], Findlater et al. [23], and Lancaster and Baas [24] based on different vegetation types. The soil cover percentage is different from the roughness effect from the silhouette shape of vegetation density, even though they expect to correlate [25].

The amount of residue and the cohesion of a surface is dependent on the crop and land use type, and the harvesting and cultivation technique [19,26–29]. These surface conditions then also rely on favourable annual weather conditions. For example, droughts can result in higher amounts of fallow lands since this can result in crop failure. Farmers can also decide to keep a field unplanted during a drought. Despite the general knowledge on the relationship between surface conditions and surface erodibility, the relationship between crop and land management, and field erodibility is often missing.

The percentage of soil cover has often been quantified by image analyses from photos in wind tunnel studies [16,30] or by certain formulas that combine the dimensions and densities of the plant [24,31]. However, image analyses from manually taken pictures are only suitable for small scale measurements, and formulas depend largely on the type and the maturity of the vegetation. A new method to determine the soil cover is the image analyses of Unmanned Aerial Vehicle (UAV) images, since this had the precision of image analyses but can cover larger areas. The feasibility of using UAV analyses to determine the soil cover has been demonstrated by Zhang et al. [32] but has not been used often.

One region that experiences high-intensity wind erosion is the Free State province in South Africa, where the majority of the dust sources can be linked to agricultural land [33]. Roughly a third of the land in the Free State is used for agriculture [34]. The dust season in this region occurs between August and November, when the fields have been harvested and often ploughed in preparation for the beginning of the rainy season in December. The amount of dust events varies greatly per year [33], which raises the question of which other factors influence the emission of dust in the Free State, and to which extent these factors can be controlled by agricultural management.

Maize is the most common crop in the Free State, but depending on the soil and climate, also other crops such as sunflower, soya beans, wheat, sorghum, and groundnuts are cultivated. Furthermore, a significant number of fields is fallow. Fallow fields can either be a conscious decision to increase the water level or the result of low or late rains, causing farmers to miss the window of seeding [35]. Figure 1 shows the average land use from an average rainfall of 487 mm per year, and the land use during the drought in 2015–2016 when only 294 mm rainfall fell. These figures show the importance of maize as the main crop in this region and the increase in fallow fields during drought.

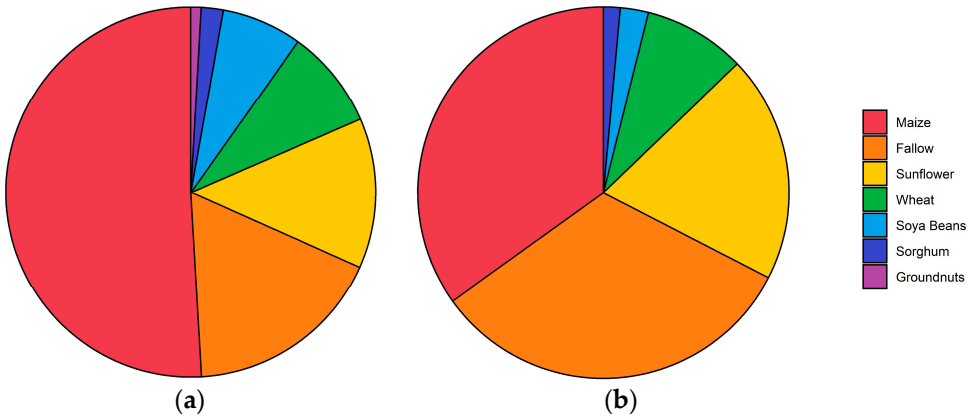

Figure 1. The land use in the Free State on average from 2006 to 2017 (**a**) and during the drought year of 2015–2016 (**b**). Data provided by the South African Department of Agriculture, Fisheries and Forestry (DAFF).

In the Free State, especially groundnut and fallow fields have been linked with wind erosion and dust events. Local farmers have indicated that groundnut fields show the highest intensity in wind erosion. Furthermore, Eckardt et al. [33] connected a year with a high number of dust source points with the large number of fallow areas that were caused by drought. The number of fallow fields does show a relationship with the rainfall with an R^2 value of 0.15 (Figure 2). However, Vos et al. [36] measured a low dust emission flux on

these fields as long as the presence of sandy saltators and abrasion are limited, due to the crusted nature and high cohesion of these fields.

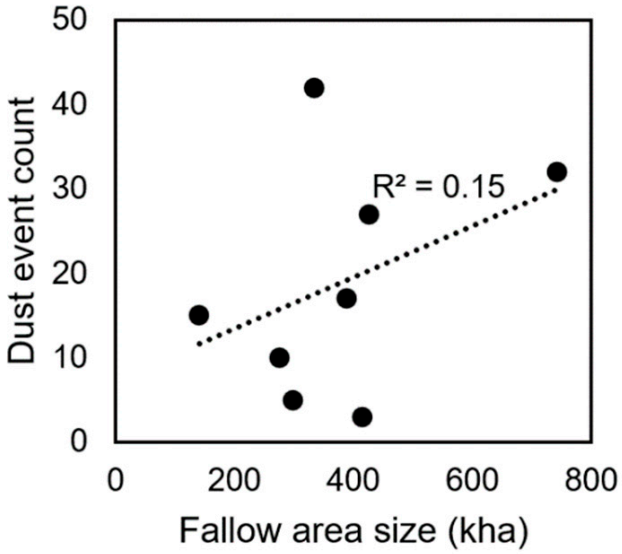

Figure 2. The yearly fallow area size versus the dust event count. Data from Eckardt et al. [33] and the Department of Agriculture, Forestry and Fisheries (DAFF).

The question of the factors influencing the dust emissions in this region has been raised previously by Vos et al. [36]. Using the Portable In Situ Wind Erosion Laboratory (PI-SWERL), they identified the presence of a crust to be an important factor in minimizing emission. In addition, the texture of a loose surface affected the PM_{10} emission flux greatly. However, the PI-SWERL is too small to capture the influence of the plant cover and the roughness from ploughing ridges or stubble. Wiggs et al. [37] monitored the erosion from a ploughed bare field in the Free State using saltation sensors, anemometers, and dust deposition traps and found a correlation between roughness and the threshold velocity. They furthermore described the minor role of moisture and rainfall in minimizing emission due to high wind velocities during similar periods. However, both of these studies do not address the influence of plant cover and stubble.

This study aims at quantifying wind erosion on a range of the most common field conditions encountered on Free State cropland during the dust season and at developing an understanding of the land management and cropping systems that potentially generate most wind erosion and dust emission in this region. To address this, the sediment flux and threshold velocity of four fields with typical combinations of cover and surface characteristics were measured. The monitored surface characteristics consist of cohesion, soil cover, and roughness. The soil erodibility is described by the threshold velocity and the horizontal sediment flux. The objectives of this study are to determine the following:

1. The surface characteristics of the fields;
2. The sediment flux and threshold velocity on the different fields during the dust season;
3. The influence of the field characteristics on the soil erodibility;
4. A wind erosion risk assessment associated with different land use.

2. Materials and Methods

2.1. Study Area and Sites

The study area is located in the northwestern part of the Free State (Figure 3), a region that shows the most dust source points as described by Eckardt et al. [33]. A climate station from the Agricultural Research Council (ARC) provided hourly data on the weather conditions (Figure 3). The rainfed agriculture in this mainly semi-arid region is largely sustained by the deep, sandy Arenosol and Luvisol, as classified using the Soil Atlas of

Africa [38]. Such soils commonly have an infiltration rate between 15 and 70 mm h^{-1}, depending on the moisture content, soil chemistry, and the stage of tillage or compaction throughout the cropping cycle [39,40]. The sandy soils in the Free State can function as a water reservoir [41]. No irrigation is taking place on these fields, which makes the agriculture highly dependent on favourable rainfall conditions. The seeding of the crop starts at the beginning of the rainy season in early spring [35], except for winter wheat which is planted during fall due to its frost resistance [42].

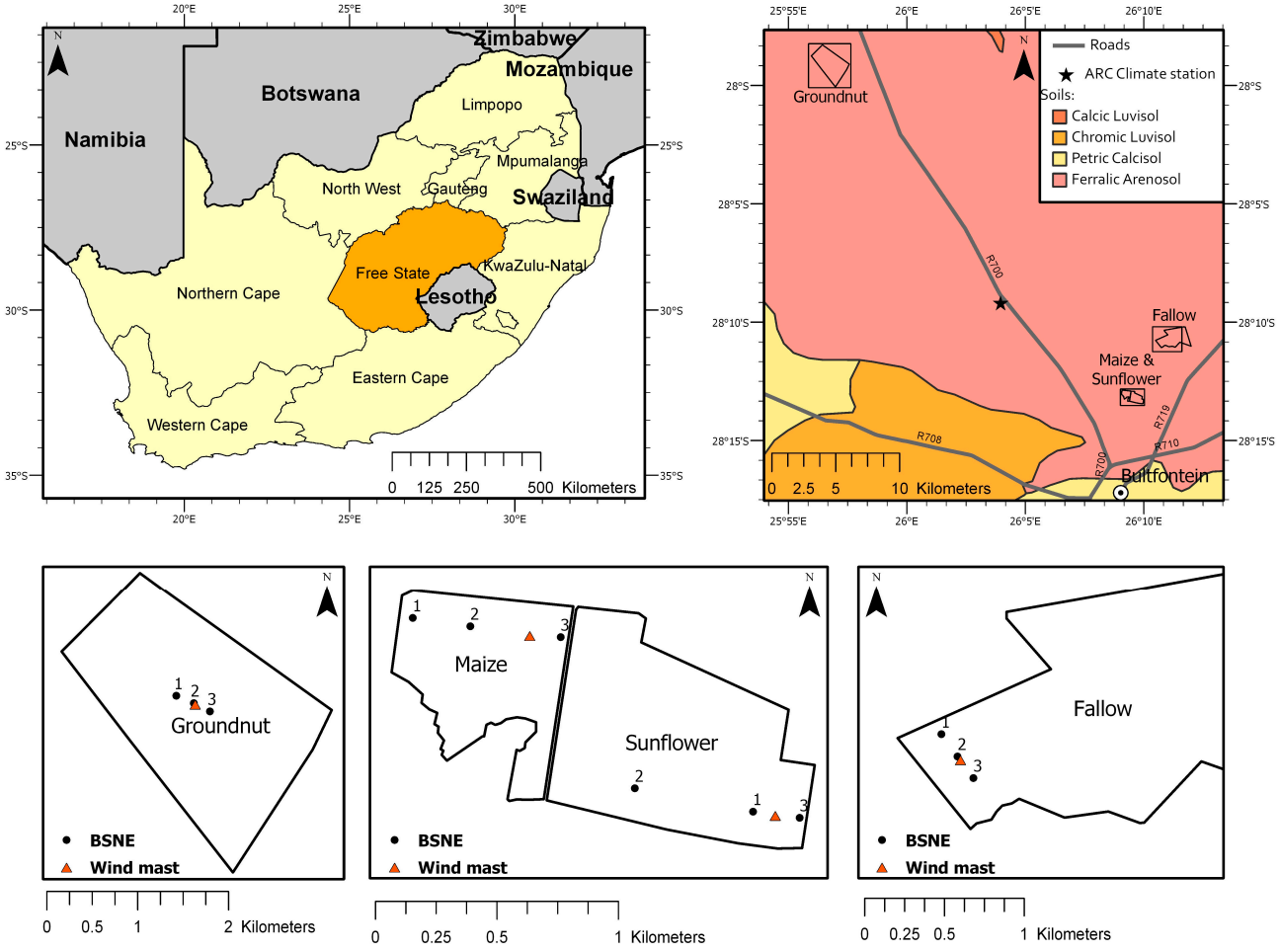

Figure 3. South Africa (**top left**), the soil map of the study area (**top right**), and the fields that were selected for monitoring (**bottom**) with the location of the Big Spring Number Eight (BSNE) and wind masts.

Four fields, representing the most important fields and crop types and showing a range of soil cover and cohesion conditions were monitored (Figures 3 and 4). The selected fields are a harvested maize, a sunflower, a groundnut and a fallow field. Maize and sunflower constitute over 90% of the crop production in the region and thus leave the largest proportion of cropland exposed to potentially erosive winds after harvest [34]. Groundnut and fallow fields have been linked to higher wind erosion risks.

The height of the stubble on the different fields is described in Table 1. All fields except for the fallow field were planted in January and harvested in July and August. No further tillage or cultivation has been performed on these fields yet. The maize field was a harvest field that had still standing straw and stubble after harvesting. The bare soil of this field was partially crusted and partially disturbed by tracks. The sunflower field was a harvested sunflower field with standing and laying stubble and had rows of low plant stubble, crusted rows, and track rows. The groundnut field was a harvested groundnut

field with a mainly loose soil surface caused by the full removal of the crop and mechanical breakup of the soils during harvest. This field was furthermore largely covered by sand deposits that showed signs of wind erosion. Vos et al. [36] showed that these sand deposits are depleted in fines. The fallow field was a maize field that had not been planted during the past rainy season, causing the maize stubble from the year before to deteriorate. This resulted in a much lower soil cover than the maize field, but a fully crusted surface. Despite the lack of agricultural activities, this field still showed significant ridges and furrows, attributed to past seeding operations.

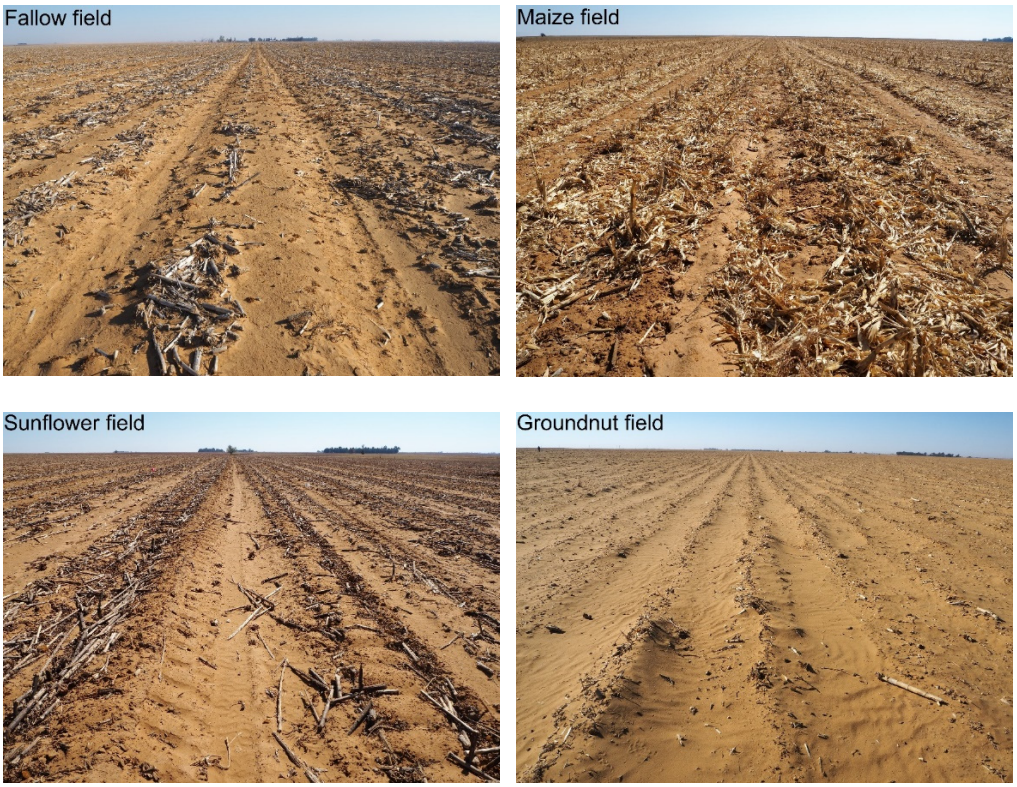

Figure 4. The four fields that were monitored during the field study.

Table 1. The height from the laying and standing stubble of the four fields.

Field	Stubble Laying	Stubble Standing
Sunflower	2–5 cm	10 to 20 cm
Maize	0–10 cm	30 cm
Peanut	0–2 cm	None
Fallow	None	None

The soil type of all fields in this study is an Arenosol, which is a prominent type in the Free State and commonly used for high-intensity agriculture [41]. Arenosols make up 15.3% of the soil area of South Africa. The texture of the soils ranged from loamy sand to sandy loam (Table 2).

Table 2. The average soil texture and Total Organic Carbon (TOC) content of the four fields.

Field	Average Clay %	Average Silt %	Average Sand %	Average TOC %
Maize field	12.3	3.0	84.7	0.227
Sunflower field	10.2	2.7	87.1	0.200
Groundnut field	8.7	2.6	88.8	0.184
Fallow field	17.1	4.1	78.8	0.318

2.2. Experimental Design

In each field, an anemometer mast, three Big Spring Number Eight (BSNE) masts, and a Sensit sensor were installed, see Figure 3. The fields were monitored from 26 August to 23 September.

BSNE sediment samples were used [43] to get an indication of the sediment flux during the period of monitoring. This is a commonly used sediment sampler due to its low cost, high efficiency, and general stability at different wind velocities [43–45]. Per field, three BSNE masts were installed (Figure 3) in a line following the observed soil texture gradient in the field to capture the within-field variations. The masts were positioned at a distance of 200 to 500 m from each other. The sediment was sampled after each wind event day, but the sediment flux is only calculated from the entire field monitoring period.

The data collected by the traps enable the calculation of the sediment transport and allow a general comparison between the fields. However, it will not give us precise insight into the spatial variability of a field since this would have required a much higher number of sampling positions, as discussed by [46,47]. Each mast held three BSNEs at 0.10, 0.35, and 0.60 m height, defined from the geometric mean of the opening as proposed by Ellis et al. [48]. These heights were determined by the minimal possible distance of the lowest sampler to the ground, and of the minimal possible distance from the samplers to each other. The BSNE samples were weighted with a scale with a precision of 0.01 g. The efficiency of the BSNE correlates positively with the grainsize [44,45,49]. Since the efficiency of saltating grains is described to be near 100% [18,44], we will assume this efficiency for the horizontal mass flux samples.

During the field monitoring, wind velocity and direction were also observed, from which the aerodynamic roughness length of each field was calculated (see Section 2.3.2). The wind velocity and directions were monitored using Davis cup anemometers (Decagon Devices, Inc., Pullman, WA 99163, USA) attached to Decagon ZL6 loggers. These anemometers measure the wind velocity and wind direction with a precision of 5% and 7°, respectively, at a minimum of 0.9 m s^{-1} and a one-minute interval. Four anemometers were installed on a wind mast at 0.25, 0.5, 0.85, and 1.65 m height to measure the logarithmic wind profile.

The threshold of wind erosion is often regarded as an important indicator of the erodibility of a surface [50–54]. In order to detect this threshold for the monitored sites, the saltation was monitored using the Sensit TM-H14-LIN (Sensit Inc., Redlands, CA 92374, USA). This instrument uses a cylindrical piezo-electric cylinder that counts the impact of saltating grains. The advantage of the Sensit is its sensitivity to smaller particles and low wind velocities. Van Pelt et al. [55] described the threshold diameter size of the Sensit to be below 125 mm for a wind velocity of 7.5 m s^{-1}. It has been used by several field- and wind tunnel studies [13,44,45,49,56] to measure the saltation threshold. The Sensit data were recorded using the Campbell CR300 data logger and combined with the wind velocity measured at 1.65 m. Both values were aggregated to an interval with a one-minute interval. Two Sensit sensors were used to monitor four fields, therefore, positioning had to be alternated. Consequently, the saltation activity was only recorded partially. The Sensit sensor was installed close to the wind mast as shown in Figure 3.

2.3. Computation of Parameters

2.3.1. Sediment Flux

The mass data from the BSNEs is transformed to a horizontal sediment flux. For these calculations, we will use a power relationship as proposed by Zobeck and Fryrear [57] as well as others, Abdourhamane Toure et al. [18], Sharratt et al. [49], and Webb et al. [58]. Therefore, the sediment flux Q (g m^{-2}) with height z (m) is described as:

$$Q = \alpha z^{\beta} \quad (1)$$

This relationship is integrated between 0.025 and 2 m height to calculate the sediment flux Q (g m^{-2}), following the study on agricultural fields from Sharratt et al. [49]. This kind

of integration was found to be the best option, despite the risk of errors in the extrapolation of the sediment flux near the ground, especially considering the differences in roughness between the fields. The regression and heights for integration to calculate the horizontal sediment flux remains debated [48,59].

2.3.2. Aerodynamic Roughness Length

From the wind profile measured per minute by the anemometers, the aerodynamic roughness length was measured using a least-square fit on the Karman-Prandtl law-of-the-wall:

$$\frac{u_z}{u_*} = \frac{1}{k} \ln \frac{z}{z_0} \tag{2}$$

Whereby u_* is the friction velocity (m s^{-1}), u_z is the wind velocity (m s^{-1}) at height z (m), k is the von Karman constant (0.40), and z_0 is the aerodynamic roughness length (m). To calculate the aerodynamic roughness length, only measurements with a wind velocity above 0.9 m s^{-1} at the bottom anemometer were used. All the measured values were averaged per field for a final value.

2.3.3. Saltation Threshold

To calculate the threshold velocity, the time fraction equivalence method (TFEM) from Stout and Zobeck [60,61] and modified by Wiggs et al. [56] was used. This formula assumes that the fraction of time units that saltation has been recorded is the same as the fraction of time units that the threshold wind velocity has been exceeded. Therefore, the minute saltation data ($p(t)$) is turned into binary data ($b_p(t)$). This gives the following formula:

$$\gamma_p = \frac{1}{N} \sum_{i=1}^{N} b_{pi} \tag{3}$$

Here, γ_p is the intermittency function, which can be linked to a certain wind velocity, which represents the threshold velocity. As discussed by Stout and Zobeck [60], there is a negative correlation between the interval length of the measurements and the calculated threshold. Therefore, it is important to take into account that looking at second or hourly data, the threshold will be higher or lower, respectively.

2.4. Soil Cover from UAV Imagery

UAV imagery was collected during the dust season field campaign in 2019 to determine the surface area of the bare soil and the plant cover in each field. The UAV used for this study was a DJI Mavic Pro. To achieve a high resolution of the orthomosaic and digital surface model (DSM), the flight altitude was 10 m. The fields could only be partially covered, due to the large size of the fields in combination with the low flight low altitude. However, the obtained imagery is considered to generate a good index for the actual straw and stubble cover, because of the uniformity of soil properties and tillage practices. Image processing including orthorectification and production of a high-resolution orthomosaic and DSM was done with the photogrammetry software Pix4Dmapper.

The Ground Sampling Distance of the orthomosaic and DSM ranged from 3.1 mm to 4.1 mm. This enables a good distinction of features such as leaves and plant stumps. For the field cover analysis, the topographic ruggedness index (TRI) was calculated following Wilson et al. [62] and was used as additional input data. For the land cover classification, three land cover classes were used: cover, soil, and shadow. To identify these classes, a supervised random forest algorithm was implemented using R. The ground truth data was collected virtually for each field. To reduce bias in the data, spatial distribution was regarded as well as the random separation of the data into training and validation data for the model. The random forest model was trained with 70% of this ground truth data and the model output was then validated with the remaining 30%, while a minimum distance of two pixels between a training- and a validation pixel was required for the random data

separation. The model was then run using the RGB orthomosaic as well as the TRI raster as input data, resulting in classifications with an overall accuracy of above 90% for all fields. The final classification maps were made with ArcGIS and provided the basis for the statistical analyses on the distribution of land cover classes (Figure 5). For further analyses, the identified shadows were used as the error range. Lastly, for the maize and sunflower fields different row types (crop, crust, and track) were manually assigned and their spatial extent calculated.

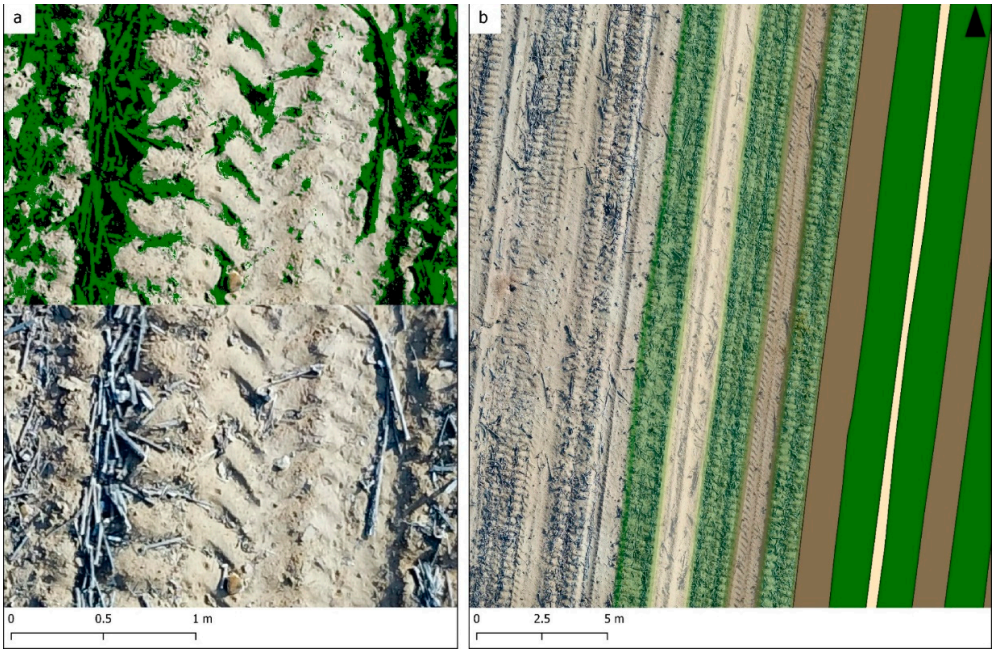

Figure 5. The results of the image analysis on the sunflower field: green represents the identified stubble cover, black represents shadow, and the remaining surface has been identified as soil (**a**). Distribution of the row types in the sunflower fields, where green is used for the planting rows, brown are the track rows, and crust is beige (**b**).

3. Results

3.1. Wind Characteristics and Sediment Flux

Figure 6 shows the wind rose for all the measured wind velocities during the period of field monitoring and the wind rose only including the velocities above the saltation threshold of 6 m s^{-1} (see Section 3.2). This wind velocity was reached during six wind events during the time of field monitoring. The general main wind direction appeared to be a southwesterly one. However, erosive winds occur in similar frequency from NE, NW, and SW direction. This is in accordance with Eckardt et al. [33] who described that the daily dust events usually come from north to westerly winds, which change into a southern and eastern direction at night. Wiggs et al. [37] also reported that most wind originates from southwestern to northwestern directions.

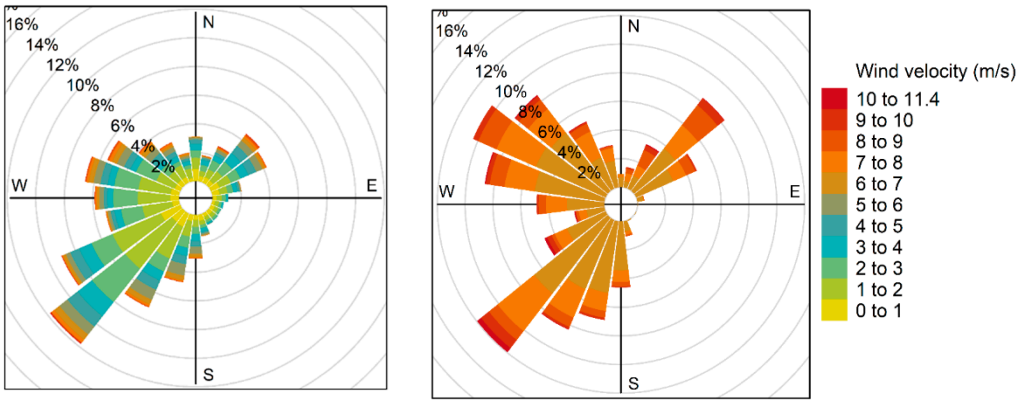

Figure 6. The wind roses from the wind data that were measured at an hour interval at the ARC climate station during the period of field monitoring of all the wind velocities (**a**) and the wind velocities above 6 m s^{-1} (**b**).

Eckardt et al. [33] used 6 m s^{-1} as the average hourly threshold velocity for dust emission. During the field monitoring, 2.3% of the hours had an average hourly wind velocity above 6 m s^{-1}, which is roughly 17 h per month. This is a percentage that is observed during most months of the dust season from 2006 to 2016. Dust events have been associated with an average maximum wind velocity of 9.8 m s^{-1}, whereas the maximum hour wind velocity during the field monitoring period was 8.15 m s^{-1}. However, dust events have also been observed at 6.7 m s^{-1}, so these lower wind velocities do not have to be regarded as irrelevant. Most important are probably gust wind velocities, which are unfortunately not recorded in the available datasets.

The calculated sediment flux that was calculated based on the BSNE traps during this period are is shown in Figure 7. The sediment flux on the groundnut field is at least 17 times larger than on the other fields. The maize field has the lowest sediment flux, followed by the sunflower field. The fallow field has on average a higher sediment flux than the sunflower field, but both fields showed a high variation in this value. This within-field variation of the sediment flux can be explained by the influence from bordering fields or changes in the erodibility in the field, as described by Bielders et al. [63], but also a certain standard variability can be expected [47].

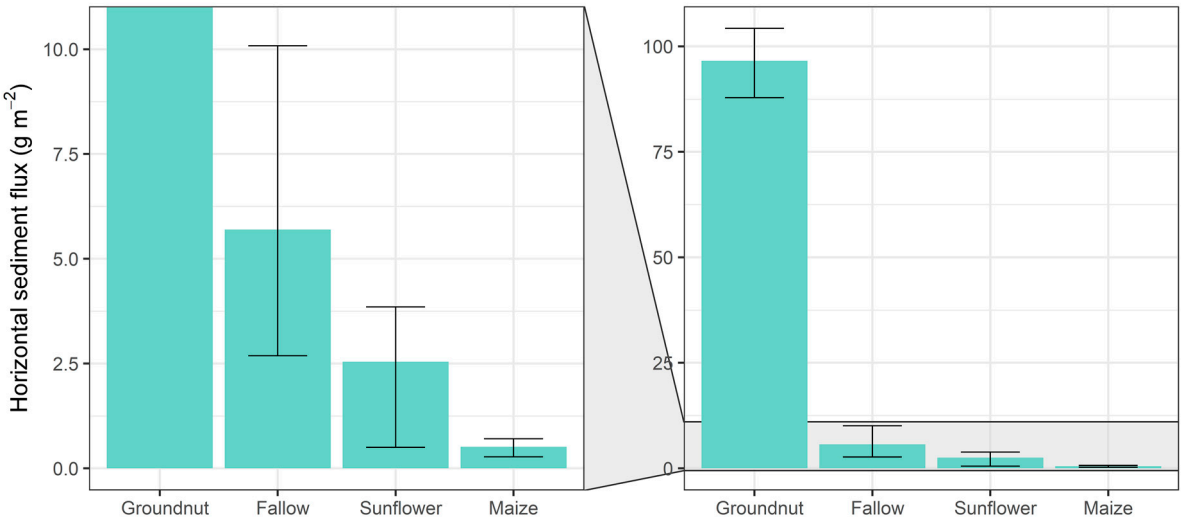

Figure 7. Average sediment flux on fields. Error bars illustrate maximum and minimum values.

3.2. Aerodynamic Roughness and Saltation Threshold

Table 3 shows the average aerodynamic roughness length and the saltation threshold velocity measured on each field. As expected, the groundnut field had the lowest aerodynamic roughness length, with a height of 0.8 mm. In contrast, the maize field had a roughness length of 31.1 mm. Somewhat surprisingly, the sunflower field and groundnut field differed only a little, despite the difference in cover. Notably, the fallow field has a higher roughness length than the sunflower field, considering the similarities in soil cover. This supports the importance of preservation of the ridge and furrow pattern for increasing aerodynamic roughness, even on fields that have not been ploughed for approximately a year.

Table 3. Measured average aerodynamic roughness length and saltation threshold velocity of the different fields.

Field	Aerodynamic Roughness Length (mm)			Saltation Threshold Velocity (m s^{-1})			Minutes That Threshold Is Exceeded (%)	Days That Threshold Is Exceeded (%)
	Mean	n	σ	Mean	n	σ		
Maize field	31.1	46	9.66	>7.7			<2.1%	<30%
Sunflower field	1.9	410	1.25	5.96	61	2.22	6.1%	45%
Groundnut field	0.8	1203	0.76	5.95	36	1.15	8.8%	62%
Fallow field	3.0	794	10.0	6.54	11	2.48	6.1%	45%

The groundnut field and sunflower field have similarly low threshold wind velocities, despite their difference in soil cover. There was no definite threshold wind velocity measured on the maize field because it was not reached during our measurement period on that field. The maximum wind velocity measured on the maize field was 7.7 m s^{-1}, leading us to assume that the threshold velocity is definitely above this value. However, it cannot be told how much higher the threshold velocity precisely is. Despite the very limited saltation, the maize field could still emit dust due to deflation. Furthermore, saltation of particles could have occurred outside of the detection range of the Sensit. This limit is 100 mm for wind velocities below 10 m s^{-1} [55], whereas particles of around 70 µm have the lowest threshold friction velocity [64]. Table 3 also shows the percentage of minutes and days that the threshold velocity is crossed. As expected, this is the highest for the groundnut field. The sunflower and fallow fields have similar values. For the maize field, only estimations can be made, assuming a minimum threshold velocity of 7.8 m s^{-1}.

3.3. Cover Percentage

The identified cover and soil percentages are shown in Table 4. As expected, the maize field has the highest soil cover, which is almost twice as high as the sunflower field and six times greater than the groundnut field. The fallow field has a cover that is comparable to the sunflower field but with a lower error from the low shadow percentage. A year ago, the soil cover on the fallow field would have been similar to the maize field. Comparing the cover percentage of the current maize field to that of the fallow field, the cover is reduced by deterioration by roughly from approximately 66% to 40%. This is a significant decrease within one year, which is expected to decrease even further when no new crop is being planted in the following year, which could be the case if, for example, a drought year occurs

Table 4. The cover and soil percentages of each field as identified by the UAV analysis.

	Maize Field		Sunflower Field		Groundnut Field		Fallow Field	
Cover	66%	±7%	38%	±5%	11%	±0.4%	40%	±0.5%
Soil	34%		62%		89%		60%	

For the maize field and sunflower field, it was possible to differentiate rows in the fields and calculate the soil cover for each row (Table 5). As expected, the soil cover was highest

for the crop rows, whereas the tracks and crusts have approximately the same soil cover percentages. This is roughly 38% for the maize field and 24% for the sunflower field. For the groundnut field and the fallow field, it was not possible to make a distinction between different rows. The cover distribution can be assumed as being rather homogenous.

Table 5. The percentage of the planting row, track, and crusts in size, and the identified surface area of each row type.

	Maize Field						Sunflower Field					
	Crop		**Crust**		**Track**		**Crop**		**Crust**		**Track**	
Fraction of field	82%		6%		12%		55%		16%		30%	
Cover	85%	±8%	39%	±7%	37%	±6%	48%	±7%	26%	±2%	22%	±3%
Soil	15%		61%		63%		52%		74%		78%	

4. Discussion

4.1. Field Characteristics

The first aim of this study was to determine the field characteristics from the maize field (high soil cover), the sunflower field (medium soil cover), the groundnut field (low soil cover), and the fallow field (medium soil cover). Our results show a positive relationship between the soil cover and the roughness (Figure 8). The groundnut field has the lowest roughness length (0.8 mm) in combination with the lowest stubble cover (11%). The maize field had a much higher roughness than the other fields (31.1 mm), which is likely related to the higher cover percentage (66%) and the height of this soil cover. The sunflower field and fallow fields are close in characteristics when it comes to roughness length (1.9 and 3.0 mm, respectively) and cover percentage (38 ± 5 and 40 ± 0.5%, respectively). The higher error in the sunflower field is caused by the relatively large area of shadow. Therefore, this field could have a higher or lower cover percentage than the fallow field depending on the surface type that the shadows in this field represent.

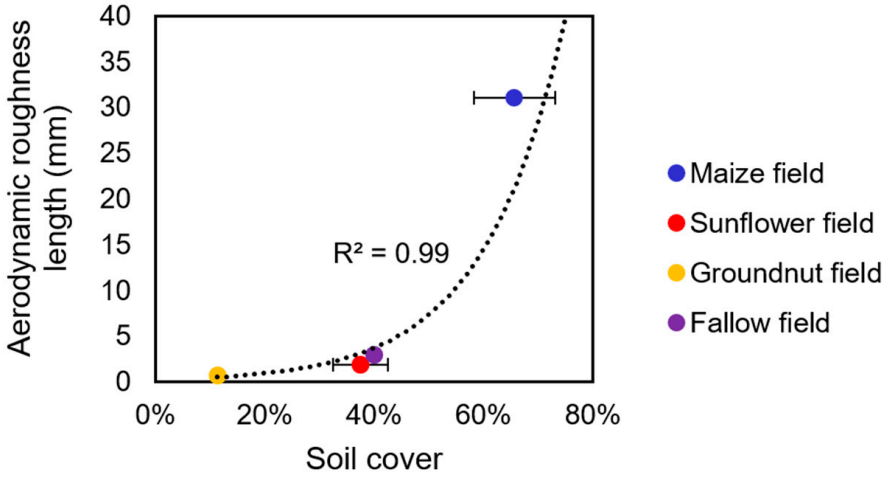

Figure 8. The soil cover versus the aerodynamic roughness length from the monitored fields.

The maize field and the sunflower field showed a spatial distribution of the soil cover, which was determined by the planting, crust and track rows. The planting rows had a much higher soil cover (85 and 48% for the maize field and sunflower field, respectively), than that on the track and crusted rows (38% and 24% on average, respective). This difference in soil cover raises the question of whether the highest, lowest, or average soil cover controls the erosion on a field within a typical pattern of surface conditions.

4.2. Erodibility and the Influence of the Field Use on Wind Erosion

The second and third aim of this study was to determine the threshold velocity and sediment flux of fields and how these values relate to the field characteristics. The threshold velocity has a positive correlation with the roughness. The estimated threshold velocity of the maize field was above 7.7 m s^{-1}, which can be explained by the high roughness and protection of the maize stubble. Cohesion is not expected to play a significant role in the threshold velocity, since the moving sand grains are expected to be loose top grains, as described by Vos et al. [65].

The sediment flux showed greater deviance between the fields than the threshold velocity and the surface characteristics, with a 117-fold difference between the groundnut field and maize field. The relationship between the soil cover and sediment flux shows a good exponential relationship as described by Funk et al. [16] and Fryrear [22,66] (Figure 9). The mentioned studies compare the sediment flux relative to the flux without soil cover, or the soil loss ratio (SLR). For our data, the soil flux of the bare soil is unknown, hence the SLR cannot be calculated. It can be expected that the soil flux from the bare soil would be different for each field, considering the difference in cohesion and roughness from ridges and furrows [53,67]. Despite the limitations of our data, the relevance of soil cover is illustrated by the observed sediment flux.

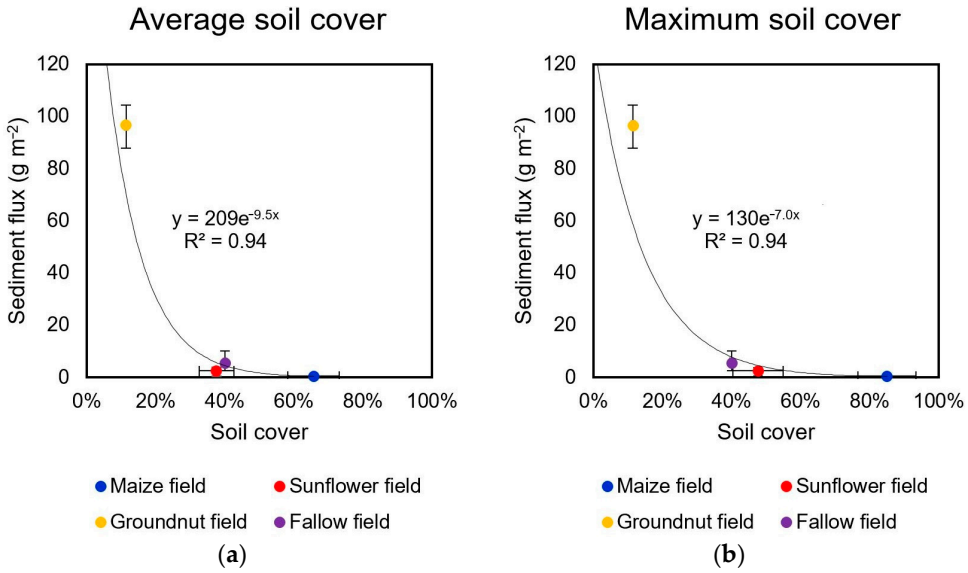

Figure 9. Relation between average sediment flux and soil cover. (**a**) Relations with average soil cover and (**b**) maximum soil cover from planting rows. The error bars indicate the variance for soil cover due to shadows in the UAV images, and the minimum and maximum value of the sediment flux.

A notable deviance from the relationship in Figure 9a is the low sediment flux on the sunflower field compared to the fallow field. This was against initial expectations, considering the higher roughness and cohesion of the fallow field. This difference could be explained by the relatively high vegetation cover in the planting rows in the sunflower field. We, therefore, hypothesize that the high plant cover in the planting rows can limit the transport from the bare rows significantly. We assume that Figure 9b, where the maximum soil cover in the rows is taken into account, is a better representation of the relationship between the soil cover and the sediment flux for the sunflower field and maize fields. Considering the NS direction of the ploughing ridges and the predominantly SW, NE, and NW wind directions, the sediment transport would be impeded across the field by the cover rich plant rows and the ploughing ridges. This would emphasize the importance of highly dense, centred vegetation rows compared to the randomized stubble in the fallow field. This effect is expected to be most pronounced when the plant row direction is at a minimum of 45° to the wind direction [16]. Another explanation for the low sediment

flux on the sunflower field could be caused by the relatively high degree of uncertainty as a result of the detected shadows from the UAV images, which could represent mainly soil cover. The maximum cover percentage on this field does show accordance with the calculated regression. This shows the limitation of UAV analyses in precisely quantifying soil cover and its influence on erodibility.

The difference between erodibility characterised by the threshold velocity and sediment flux is notable. Where the sunflower field and groundnut field had similar threshold velocities, the groundnut field had a sediment flux that was 38 times higher than the sunflower field. Furthermore, the fallow field has an average sediment flux twice as high as on the less rough sunflower field with a low threshold velocity. This difference illustrates again that the protection from cover is not just caused by the increased roughness, but also by the proportion of the surface that is covered and the spatial pattern of the cover. Both have to be considered when assessing the erodibility of a field.

The fully crusted fallow field does not show a clear influence of cohesion, since the sediment flux does plot on the regression from Figure 9 and does not show a significantly lower sediment flux. To determine the influence of crusts on the sediment flux, measurements on a field with similar cover characteristics but different levels of disturbance would be required.

4.3. Risk Assessment for Land Use Types and Implications for Dryland Agriculture

Certain land use types can have a specific range of surface characteristics that are related to the stubble quantity and cohesion of the surface. This could result in certain land-use types having a higher general wind erosion risk than others, in other words, the cover or cohesion during one crop rotation cycle alone is not sufficient to assess erodibility in situations where drought may interrupt such cycles. Considering the degrading effect of dust emission on soils, this is also important for the benefit of the crop production itself. To determine the risk of both influences, the measured sediment fluxes of these crops were multiplied by their surface area, see Figure 10. This calculation does not take any variance in the sediment flux per crop type into account, and it should be noted that the total sediment flux might not be directly linked to the vertical dust flux, as described by Sterk et al. [68]. Furthermore, data on sorghum, soybeans, and wheat are missing. Wheat is expected to have a low wind erosion risk since the growing season is in winter. Meaning that it has a very high soil cover during the dust season. The relative importance of soybeans and sorghum, which cover 9% of the agricultural land in the Free State still needs to be assessed. Nonetheless, Figure 10 shows the high relevance of groundnuts and fallow fields. This would fit with the conclusions from Eckardt et al. [33], who associated the high emissions of 2015/16 to the large proportion of fallow fields. Furthermore, the high emissions from groundnut fields in the Free State have not received any attention despite being identified as a problematic crop not just in this study, but also by Santra et al. [69].

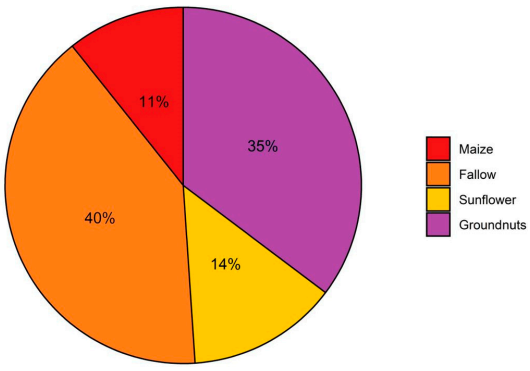

Figure 10. The relative sediment transport calculated from the average sediment flux. Note that flux data from wheat, sorghum, and soya beans are missing and that this data was excluded.

The groundnut field experienced the highest sediment flux. Considering the methods of groundnut harvest, this crop does not offer options of stubble-saving harvesting technique. Current harvesting methods destroys all crusts. The percentage of groundnut fields in the Free State is currently quite low, but the highly erosive surfaces that these crops create should be considered as potential hotspots of emissions. Other crops that leave little soil cover after harvest, such as many bean types, could pose similar risks to dust emission. The high erosion risks associated with such crops, especially in the more arid regions with erodible sandy soils, should therefore be taken into account when making land management decisions.

The cover on the fallow field originates from the deteriorated maize stubble, which created a field condition with the second-highest sediment flux. This indicates that the missing of a planting window, or the purposeful decision to do so, is a process that potentially results in a low cover that makes the field sensitive to wind erosion. The exponential relationship between soil cover and sediment flux emphasizes the even greater danger of missing the second window of planting. The sensitivity to erosion from these fallow fields would potentially become even higher if the crusts of these fields would be disturbed by tillage operations for the next rainy season.

Lastly, the maize field had a much lower sediment flux than the sunflower field, which could also be attributed to their difference in cover. This illustrates that in general, a maize straw and stubble cover offers enough protection to minimize wind erosion in the Free State. The sunflower field showed an average sediment flux that was half of that on the fallow field, making it a lower risk crop than the fallow field. Sunflower is often grown during a delayed rainy season (personal communication with farmers) and should be considered as a preferred crop compared to keeping a field fallow.

The impact of soil cohesion on emissions observed in the study of Vos et al. [36] illustrates that the preservation of crusts could be an important land management practice. In addition to conservation or reduced tillage, as described by [70–72], delaying of tillage or necessary cultivation practices could reduce dust emissions, as proposed by Funk et al. [73]. In addition to avoiding the destruction of crusts by tillage, their abrasion should also be reduced by limiting the sources of abrading sands from tracks, roads, and tillage on adjacent fields.

5. Conclusions

This study focused on characterizing the roughness and soil cover and measuring the associated wind erosion on four fields in typical Free State dust season conditions. The selected fields represent different scenarios that are common during the dust season: medium cohesion (maize field), medium cover and medium cohesion (sunflower field), high cover and low cover and low cohesion (groundnut field), and medium cover and high cohesion scenario (fallow field). This study also used UAV imagery for assessing the soil cover percentage with high resolution in the framework of a wind erosion study. The results showed a variance between 11 and 66% of soil cover. The sediment flux differed greatly among the different fields, but broadly followed a negative, exponential relationship with soil cover. The data collected at the study sites will illustrate the risk and intensity of wind erosion from different crops and field conditions. It will also provide a base to predict the behaviour of fields with different soil cover and roughness characteristics. In more general terms, this will help with the prediction of dust events and thus improve the quality of the output of wind erosion models. This study is therefore not only relevant for the Free State, but will also give an insight into factors controlling wind erosion and dust emissions on other rainfed croplands in drylands with strong seasonal contrasts in precipitation and cover [1,69,74,75].

The relationship between field condition and wind erosion observed in this study also illustrates the importance of maintaining stubble as a method to minimize wind erosion. In certain cases, the maintenance of stubble can be relatively easy, for example, by refraining from growing crops that leave little stubble after harvest such as groundnut. Maize is the

most common crop in the Free State and leaves a high straw and stubble cover and has therefore a low wind erosion risk. However, it is not always possible to grow maize because of little or late rainfall. In those cases, farmers are forced to switch to sunflower or leave a field fallow, both increasing the wind erosion risk. On a fallow field, the stubble cover will deteriorate and decline over time, in which case the focus for dust emission prevention should shift to the maintenance of soil crusts. This can involve delaying tillage operations as close as possible to the first rainfall, as well as limiting external saltators and introducing stable roughness elements such as grasslands [63,76].

Overall, the results of this study have implications for all cropland experiencing dry and windy periods outside the growing season. This raises several research questions for future research. More measurements and knowledge on the sediment flux of bare surfaces and the influence of vegetation are necessary to create a precise expression for this relationship. The influence of row width on emission appears relevant from our data, highlighting the need for studying (or at least measuring and mentioning) not just the total or average percentage of straw and stubble but, taking into account their spatial patterns. Furthermore, the erosion of crusts by abraders that may have originated outside the eroding field demonstrates that the mutual influence of neighbouring fields on their respective emissions should become a focus of wind erosion research. This involves, for example, measuring the mass balance of fallow fields and to which extent erosion can be prevented by any saltator traps on the border of a field, such as fences or grass rows. Finally, more insight into the influence of ridges from seeding and ploughing, i.e., the form roughness of the surface [37,66,67,77], on low cover fields is necessary. In such conditions, crusts in combination with tillage-induced soil surface roughness could be an important way to reduce erosion. However, the question remains whether tillage would increase emissions due to the disturbance of crusts, as suggested by Gicheru et al. [72] or decrease emission by increasing the roughness, as suggested by Wiggs et al. [37].

Author Contributions: Conceptualization, H.C.V. and N.J.K.; methodology, H.C.V., F.D.E. and N.J.K.; software, H.C.V. and I.G.K.; validation, H.C.V. and N.J.K.; formal analysis, H.C.V. and I.G.K.; investigation, H.C.V., F.D.E., W.F. and N.J.K.; resources, F.D.E. and N.J.K.; data curation, H.C.V. and I.G.K.; writing—original draft preparation, H.C.V.; writing—review and editing, F.D.E., W.F. and N.J.K.; visualization, H.C.V. and I.G.K.; supervision, N.J.K.; project administration, F.D.E. and N.J.K.; funding acquisition, F.D.E., W.F. and N.J.K. All authors have read and agreed to the published version of the manuscript.

Funding: This research was funded by the Swiss National Science Foundation (funding number IZLSZ2_170942) and the National Research Foundation (funding number 107803).

Data Availability Statement: The data presented in this study are available on request.

Acknowledgments: We would like to thank the Swiss National Science Foundation and the National Research Foundation for funding this research. We also wish to thank Hannes and Sophia Prinsloo, and A.C. van Wyk for allowing us to measure on their fields. Lastly, we would like to thank Anneliza Collett from the Department of Agriculture, Forestry and Fisheries for providing data on land use.

Conflicts of Interest: The authors declare no conflict of interest. The funders had no role in the design of the study; in the collection, analyses, or interpretation of data; in the writing of the manuscript, or in the decision to publish the results.

References

1. Sterk, G.; Riksen, M.; Goossens, D. Dryland Degradation by Wind Erosion and its Control. *Ann. Arid. Zone* **2001**, *40*, 351–367.
2. Sterk, G. Causes, consequences and control of wind erosion in Sahelian Africa: A review. *Land Degrad. Dev.* **2003**, *14*, 95–108. [CrossRef]
3. Van Pelt, R.S.; Zobeck, T.M. Chemical Constituents of Fugitive Dust. *Environ. Monit. Assess.* **2007**, *130*, 3–16. [CrossRef] [PubMed]
4. Visser, S.M.; Sterk, G. Nutrient dynamics—wind and water erosion at the village scale in the Sahel. *Land. Degrad. Dev.* **2007**, *18*, 578–588. [CrossRef]
5. Lawrence, C.; Neff, J.C. The contemporary physical and chemical flux of Aeolian dust: A synthesis of direct measurements of dust deposition. *Chem. Geol.* **2009**, *267*, 46–63. [CrossRef]

6. Zobeck, T.; Bilbro, J.D. Crop Productivity and Surface Soil Properties of a Severely Wind-Eroded Soil. In *Sustaining the Global Farm, Selected Papers from the 10th International Soil Conservation Organization Meeting*; Stott, D.E., Mohtar, R.H., Steinhardt, G.C., Eds.; ISCO: West Lafayette, IN, USA, 1999; pp. 617–622.
7. Bielders, C.L.; Rajot, J.-L.; Amadou, M. Transport of soil and nutrients by wind in bush fallow land and traditionally managed cultivated fields in the Sahel. *Geoderma* **2002**, *109*, 19–39. [CrossRef]
8. Ginoux, P.; Prospero, J.M.; Gill, T.E.; Hsu, N.C.; Zhao, M. Global-scale attribution of anthropogenic and natural dust sources and their emission rates based on MODIS Deep Blue aerosol products. *Rev. Geophys.* **2012**, *50*, 3005. [CrossRef]
9. Yang, G.; Sun, R.; Jing, Y.; Xiong, M.; Li, J.; Chen, L. Global assessment of wind erosion based on a spatially distributed RWEQ model. *Prog. Phys. Geogr. Earth Environ.* **2021**, *46*, 28–42. [CrossRef]
10. Shao, Y.P.; Wyrwoll, K.-H.; Chappell, A.; Huang, J.; Lin, Z.; McTainsh, G.H.; Mikami, M.; Tanaka, T.Y.; Wang, X.; Yoon, S. Dust cycle: An emerging core theme in Earth system science. *Aeolian Res.* **2011**, *2*, 181–204. [CrossRef]
11. Tegen, I.; Werner, M.; Harrison, S.P.; Kohfeld, K.E. Relative importance of climate and land use in determining present and future global soil dust emission. *Geophys. Res. Lett.* **2004**, *31*, L05105. [CrossRef]
12. Woodruff, N.P.; Siddoway, F.H. A Wind Erosion Equation. *Soil Sci. Soc. Am. J.* **1965**, *29*, 602–608. [CrossRef]
13. Fryrear, D.W.; Saleh, A.; Bilbro, J.D.; Schromberg, H.M.; Stout, J.E.; Zobeck, T.M.; Schomberg, H.M.; Stout, J.E.; Zobeck, T.M. *Revised Wind Erosion Equation*; United States Department of Agriculture: Big Spring, TX, USA, 1998.
14. Riksen, M.; Brouwer, F.; de Graaff, J. Soil conservation policy measures to control wind erosion in northwestern Europe. *Catena* **2003**, *52*, 309–326. [CrossRef]
15. Lyles, L. Predicting and Controlling Wind Erosion. *Agric. Hist.* **1985**, *59*, 205–214.
16. Funk, R.; Engel, W. Investigations with a field wind tunnel to estimate the wind erosion risk of row crops. *Soil Tillage Res.* **2015**, *145*, 224–232. [CrossRef]
17. Tibke, G. 5. Basic principles of wind erosion control. *Agric. Ecosyst. Environ.* **1988**, *22–23*, 103–122. [CrossRef]
18. Toure, A.A.; Rajot, J.-L.; Garba, Z.; Marticorena, B.; Petit, C.; Sebag, D. Impact of very low crop residues cover on wind erosion in the Sahel. *Catena* **2011**, *85*, 205–214. [CrossRef]
19. López, M.V.; Gracia, R.; Arrúe, J.L. Effects of reduced tillage on soil surface properties affecting wind erosion in semiarid fallow lands of Central Aragón. *Eur. J. Agron.* **2000**, *12*, 191–199. [CrossRef]
20. Li, H.; Tatarko, J.; Kucharski, M.; Dong, Z. PM2.5 and PM10 emissions from agricultural soils by wind erosion. *Aeolian Res.* **2015**, *19*, 171–182. [CrossRef]
21. Fister, W.; Ries, J.B. Wind erosion in the central Ebro Basin under changing land use management. Field experiments with a portable wind tunnel. *J. Arid Environ.* **2009**, *73*, 996–1004. [CrossRef]
22. Fryrear, D.W. Soil Cover and Wind Erosion. *Trans. ASAE* **1985**, *28*, 781–784. [CrossRef]
23. Findlater, P.A.; Carter, D.J.; Scott, B. A model to predict the effects of prostrate ground cover on wind erosion. *Aust. J. Soil Res.* **1990**, *28*, 609–622. [CrossRef]
24. Lancaster, N.; Baas, A. Influence of vegetation cover on sand transport by wind: Field studies at Owens Lake, California. *Earth Surf. Process. Landf.* **1998**, *23*, 69–82. [CrossRef]
25. Bilbro, J.D.; Fryrear, D.W. Wind Erosion Losses as Related to Plant Silhouette and Soil Cover. *Agron. J.* **1994**, *86*, 550–553. [CrossRef]
26. Nordstrom, K.F.; Hotta, S. Wind erosion from cropland in the USA: A review of problems, solutions and prospects. *Geoderma* **2004**, *121*, 157–167. [CrossRef]
27. Nelson, R.G. Resource assessment and removal analysis for corn stover and wheat straw in the Eastern and Midwestern United States—rainfall and wind-induced soil erosion methodology. *Biomass Bioenergy* **2002**, *22*, 349–363. [CrossRef]
28. Lin, X.; Niu, J.; Yu, X.; Berndtsson, R.; Wu, S.; Xie, S. Maize residue effects on PM2.5, PM10, and dust emission from agricultural land. *Soil Tillage Res.* **2021**, *205*, 104738. [CrossRef]
29. Yang, C.; Geng, Y.; Fu, X.Z.; Coulter, J.A.; Chai, Q. The Effects of Wind Erosion Depending on Cropping System and Tillage Method in a Semi-Arid Region. *Agronomy* **2020**, *10*, 732. [CrossRef]
30. Burri, K.; Gromke, C.; Lehning, M.; Graf, F. Aeolian sediment transport over vegetation canopies: A wind tunnel study with live plants. *Aeolian Res.* **2011**, *3*, 205–213. [CrossRef]
31. Li, J.; Okin, G.S.; Alvarez, L.; Epstein, H. Quantitative effects of vegetation cover on wind erosion and soil nutrient loss in a desert grassland of southern New Mexico, USA. *Biogeochemistry* **2007**, *85*, 317–332. [CrossRef]
32. Zhang, J.; Guo, W.; Zhou, B.; Okin, G.S. Drone-Based Remote Sensing for Research on Wind Erosion in Drylands: Possible Applications. *Remote Sens.* **2021**, *13*, 283. [CrossRef]
33. Eckardt, F.D.; Bekiswa, S.; Von Holdt, J.; Jack, C.; Kuhn, N.J.; Mogane, F.; Murray, J.E.; Ndara, N.; Palmer, A. South Africa's agricultural dust sources and events from MSG SEVIRI. *Aeolian Res.* **2020**, *47*, 100637. [CrossRef]
34. DAFF. *Abstract of Agricultural Statistics*; Department of Agriculture, Forestry and Fisheries: Pretoria, South Africa, 2018.
35. Moeletsi, M.E.; Walker, S. Rainy season characteristics of the Free State Province of South Africa with reference to rain-fed maize production. *Water SA* **2012**, *38*, 775–782. [CrossRef]
36. Vos, H.C.; Fister, W.; von Holdt, J.R.; Eckardt, F.D.; Palmer, A.R.; Kuhn, N.J. Assessing the PM10 emission potential of sandy, dryland soils in South Africa using the PI-SWERL. *Aeolian Res.* **2021**, *53*, 100747. [CrossRef]

37. Wiggs, G.F.S.; Holmes, P. Dynamic controls on wind erosion and dust generation on west-central Free State agricultural land, South Africa. *Earth Surf. Process. Landf.* **2011**, *36*, 827–838. [CrossRef]
38. Jones, A.; Breuning-Madsen, H.; Brossard, M.; Dampha, A.; Deckers, J.; Dewitte, O.; Gallali, T.; Hallett, S.; Jones, R.; Kilasara, M.; et al. *Soil Atlas of Africa*; European Commission, Publications Office of the European Union: Luxembourg, 2013; ISBN 978-92-79-26715-4.
39. Meek, B.D.; Rechel, E.R.; Carter, L.M.; DeTar, W.R.; Urie, A.L. Infiltration Rate of a Sandy Loam Soil: Effects of Traffic, Tillage, and Plant Roots. *Soil Sci. Soc. Am. J.* **1992**, *56*, 908–913. [CrossRef]
40. Patle, G.T.; Sikar, T.T.; Rawat, K.S.; Singh, S.K. Estimation of infiltration rate from soil properties using regression model for cultivated land. *Geol. Ecol. Landsc.* **2019**, *3*, 1–13. [CrossRef]
41. Hensley, M.; Le Roux, P.; Preez, C.D.U.; van Huyssteen, C.W.; Kotze, E.; Van Rensburg, L. Soils: The Free State's Agricultural Base. *S. Afr. Geogr. J.* **2006**, *88*, 11–21. [CrossRef]
42. DAFF. *Production Guidline for Wheat*; Department of Agriculture, Forestry and Fisheries: Pretoria, South Africa, 2016.
43. Fryrear, D.W. A field dust sampler. *J. Soil Water Conserv.* **1986**, *41*, 117–120.
44. Goossens, D.; Offer, Z.Y. Wind tunnel and field calibration of six aeolian dust samplers. *Atmos. Environ.* **2000**, *34*, 1043–1057. [CrossRef]
45. Yang, X.; Wang, M.; He, Q.; Mamtimin, A.; Huo, W.; Yang, F.; Zhou, C. Estimation of sampling efficiency of the Big Spring Number Eight (BSNE) sampler at different heights based on sand particle size in the Taklimakan Desert. *Geomorphology* **2018**, *322*, 89–96. [CrossRef]
46. Klose, M.; Gill, T.E.; Etyemezian, V.; Nikolich, G.; Ghodsi Zadeh, Z.; Webb, N.P.; Van Pelt, R.S. Dust emission from crusted surfaces: Insights from field measurements and modelling. *Aeolian Res.* **2019**, *40*, 1–14. [CrossRef]
47. Webb, N.P.; Chappell, A.; Edwards, B.L.; McCord, S.E.; Van Zee, J.W.; Cooper, B.F.; Courtright, E.M.; Duniway, M.C.; Sharratt, B.S.; Tedela, N.; et al. Reducing Sampling Uncertainty in Aeolian Research to Improve Change Detection. *J. Geophys. Res. Earth Surf.* **2019**, *124*, 1366–1377. [CrossRef]
48. Ellis, J.T.; Li, B.; Farrell, E.J.; Sherman, D.J. Protocols for characterizing aeolian mass-flux profiles. *Aeolian Res.* **2009**, *1*, 19–26. [CrossRef]
49. Sharratt, B.S.; Feng, G.; Wendling, L. Loss of soil and PM10 from agricultural fields associated with high winds on the Columbia Plateau. *Earth Surf. Process. Landf.* **2007**, *32*, 621–630. [CrossRef]
50. Fryrear, D.W.; Stout, J.E.; Hagen, L.J.; Vories, E.D. Wind Erosion: Field Measurement and Analysis. *Trans. ASAE* **1991**, *34*, 155–160. [CrossRef]
51. Li, J.; Okin, G.S.; Herrick, J.; Belnap, J.; Munson, S.; Miller, M.E. A simple method to estimate threshold friction velocity of wind erosion in the field. *Geophys. Res. Lett.* **2010**, *37*, L10402. [CrossRef]
52. Sharratt, B.S.; Vaddella, V. Threshold friction velocity of crusted windblown soils in the Columbia Plateau. *Aeolian Res.* **2014**, *15*, 227–234. [CrossRef]
53. Gillette, D.A. Threshold friction velocities for dust production for agricultural soils. *J. Geophys. Res. Atmos.* **1988**, *93*, 12645–12662. [CrossRef]
54. Gillette, D.A.; Adams, J.; Endo, A.; Smith, D.; Kihl, R. Threshold velocities for input of soil particles into the air by desert soils (Mojave). *J. Geophys. Res.* **1980**, *85*, 5621–5630. [CrossRef]
55. Van Pelt, R.S.; Peters, P.; Visser, S.M. Laboratory wind tunnel testing of three commonly used saltation impact sensors. *Aeolian Res.* **2009**, *1*, 55–62. [CrossRef]
56. Wiggs, G.F.S.; Baird, A.J.; Atherton, R.J. The dynamic effects of moisture on the entrainment and transport of sand by wind. *Geomorphology* **2004**, *59*, 13–30. [CrossRef]
57. Zobeck, T.M.; Fryrear, D.W. Chemical and Physical Characteristics of Windblown Sediment II. Chemical Characteristics and Total Soil and Nutrient Discharge. *Trans. ASAE* **1986**, *29*, 1037–1041. [CrossRef]
58. Webb, N.P.; Strong, C.L.; Chappell, A.; Marx, S.K.; McTainsh, G.H. Soil organic carbon enrichment of dust emissions: Magnitude, mechanisms and its implications for the carbon cycle. *Earth Surf. Process. Landf.* **2013**, *38*, 1662–1671. [CrossRef]
59. Mendez, M.J.; Funk, R.; Buschiazzo, D.E. Field wind erosion measurements with Big Spring Number Eight (BSNE) and Modified Wilson and Cook (MWAC) samplers. *Geomorphology* **2011**, *129*, 43–48. [CrossRef]
60. Stout, J.E.; Zobeck, T.M. Intermittent saltation. *Sedimentology* **1997**, *44*, 959–970. [CrossRef]
61. Stout, J.E.; Zobeck, T.M. The Wolfforth Field Experiment: A Wind Erosion Study. *Soil Sci.* **1996**, *161*, 616–632. [CrossRef]
62. Wilson, M.F.J.; O'Connell, B.; Brown, C.; Guinan, J.C.; Grehan, A.J. Multiscale Terrain Analysis of Multibeam Bathymetry Data for Habitat Mapping on the Continental Slope. *Mar. Geod.* **2007**, *30*, 3–35. [CrossRef]
63. Bielders, C.L.; Vrieling, A.; Rajot, J.-L.; Skidmore, E.L. On-farm evaluation of field-scale soil losses by wind erosion under traditional management in the Sahel. Soil erosion research for the 21st century. In proceedings of the International Symposium, Honolulu, HI, USA, 3–5 January 2001. [CrossRef]
64. Greeley, R.; Iversen, J.D. *Wind as a Geological Process on Earth, Mars, Venus and Titan*; Cambridge University Press: Cambridge, UK, 1985; ISBN 9780521359627.
65. Vos, H.C.; Fister, W.; Eckardt, F.D.; Palmer, A.; Kuhn, N.J. Physical Crust Formation on Sandy Soils and Their Potential to Reduce Dust Emissions from Croplands. *Land* **2020**, *9*, 503. [CrossRef]
66. Fryrear, D.W. Soil Ridges-Clods and Wind Erosion. *Trans. ASAE* **1984**, *27*, 445–448. [CrossRef]

67. Liu, M.-X.; Wang, J.-A.; Yan, P.; Liu, L.-Y.; Ge, Y.-Q.; Li, X.-Y.; Hu, X.; Song, Y.; Wang, L. Wind tunnel simulation of ridge-tillage effects on soil erosion from cropland. *Soil Tillage Res.* **2006**, *90*, 242–249. [CrossRef]
68. Sterk, G.; Herrmann, L.; Bationo, A. Wind-blown nutrient transport and soil productivity changes in southwest Niger. *Land Degrad. Dev.* **1996**, *7*, 325–335. [CrossRef]
69. Santra, P.; Moharana, P.C.; Kumar, M.; Soni, M.L.; Pandey, C.B.; Chaudhari, S.K.; Sikka, A.K. Crop production and economic loss due to wind erosion in hot arid ecosystem of India. *Aeolian Res.* **2017**, *28*, 71–82. [CrossRef]
70. Pi, H.; Sharratt, B.S.; Schillinger, W.F.; Bary, A.I.; Cogger, C.G. Wind erosion potential of a winter wheat–summer fallow rotation after land application of biosolids. *Aeolian Res.* **2018**, *32*, 53–59. [CrossRef]
71. Sharratt, B.S.; Collins, H.P. Wind Erosion Potential Influenced by Tillage in an Irrigated Potato–Sweet Corn Rotation in the Columbia Basin. *Agron. J.* **2018**, *110*, 842–849. [CrossRef]
72. Gicheru, P.; Gachene, C.; Mbuvi, J.; Mare, E. Effects of soil management practices and tillage systems on surface soil water conservation and crust formation on a sandy loam in semi-arid {Kenya}. *Soil Tillage Res.* **2004**, *75*, 173–184. [CrossRef]
73. Funk, R.; Reuter, H.; Hoffmann, C.; Engel, W.; Oettl, D. Effect of Moisture on Fine Dust Emission from Tillage Operations on Agricultural Soils. *Earth Surf. Proc. Land.* **2008**, *33*, 1851–1863. [CrossRef]
74. López, M.V.; Sabre, M.; Gracia, R.; Arrúe, J.L.; Gomes, L. Tillage effects on soil surface conditions and dust emission by wind erosion in semiarid {Aragón} ({NE} {Spain}). *Soil Tillage Res.* **1998**, *45*, 91–105. [CrossRef]
75. Bunn, J.A. Government Policy, Wind Erosion, And Economic Viability In Semi-Arid Agriculture: The Case Of The Southern Texas High Plains. *J. Agric. Appl. Econ.* **1998**, *30*, 339–351. [CrossRef]
76. Rajot, J.-L. Wind blown sediment mass budget of Sahelian village land units in Niger. *Bull. Soc. Géol. Fr.* **2001**, *172*, 523–531. [CrossRef]
77. Raupach, M.R.; Gillette, D.A.; Leys, J.F. The effect of roughness elements on wind erosion threshold. *J. Geophys. Res. Atmos.* **1993**, *98*, 3023–3029. [CrossRef]